

**IMPLICATIONS FOR METALLOGRAPHIC COOLING RATES, DERIVED FROM FINE-SCALE ANALYTICAL TRAVERSES ACROSS KAMACITE, TAENITE, AND TETRATAENITE IN THE BUTLER IRON METEORITE.** J.H. Jones<sup>1</sup>, D.K. Ross<sup>2</sup>, N.L. Chabot<sup>3</sup>, and L.P. Keller<sup>1</sup>. <sup>1</sup>XI-3, NASA/JSC, Houston, TX 77058 (john.h.jones@nasa.gov), <sup>2</sup>Jacobs JETS, NASA/JSC, Houston, TX 77058. <sup>3</sup>Johns Hopkins University Applied Physics Laboratory, Laurel, MD 20723.

**Introduction:** The “M-shaped” Ni concentrations across Widmanstätten patterns in iron meteorites, mesosiderites, and ordinary chondrites are commonly used to calculate cooling rates [e.g., 1-3]. As Ni-poor kamacite evolves from Ni-rich taenite, Ni concentrations build up at the kamacite-taenite interface because of the sluggish diffusivity of Ni. Quantitative knowledge of experimentally-determined Ni diffusivities, coupled with the shape of the M-profile, have been used to allow calculation of cooling rates that pertained at low temperatures,  $\leq 500^\circ\text{C}$ .

However, determining Ni metallographic cooling rates are challenging, due to the sluggish diffusivity of Ni at low temperatures. There are three potential difficulties in using Ni cooling rates at low temperatures: (i) Ni diffusivities are typically extrapolated from higher-temperature measurements [3]; (ii) Phase changes occur at low temperatures that may be difficult to take into account [3]; and (iii) It appears that Ge in kamacite and taenite has continued to equilibrate (or attempted to equilibrate) at temperatures below those that formed the M-shaped Ni profile [4].

Combining Ni measurements with those of other elements has the potential to provide a way to confirm or challenge Ni-determined cooling rates, as well as provide insight into the partitioning behaviors of elements during the cooling of iron meteorites. Despite these benefits, studies that examine elemental profiles of Ni along with other elements in iron meteorites are limited, often due to the low concentration levels of the other elements and associated analytical challenges. The Butler iron meteorite provides a good opportunity to conduct a multi-element analytical study, due to the higher concentration levels of key elements in addition to Fe and Ni. In this work, we perform combined analysis for six elements in the Butler iron to determine the relative behaviors of these elements during the evolution of iron meteorites, with implications for metallographic cooling rates.

**The Butler Iron:** Butler is classified as an anomalous iron meteorite, which is believed to be related to NWA 859 (J. T. Wasson, pers. comm.). It was chosen for study because of its high Ge content and because high-precision Ge traverses had already been performed [4].

**Analytical:** Analytical traverses for Fe, Ni, Co, Ge, Cu, and Ga were performed across a kamacite band and its adjacent tetrataenite and taenite zones. The

length of each traverse was about  $52\mu$ . The first traverse analyzed for Fe, Ni, Co, Ge and the second traverse emphasized Cu and Ga. Analyses were performed using a FEG JEOL JXA 8530F electron microprobe. Step distance for the first traverse was  $0.8\mu$  and was  $1.1\mu$  for the second traverse. The first traverse was collected at 15 kV and 100 nA, and the second traverse was collected at 20 kV and 200 nA. We analyzed for the Ge  $L_\alpha$  using a TAP crystal and the Ga, Cu, Fe, Ni, and Co  $K_\alpha$  lines were measured using an LIF crystal. Cobalt analyses were corrected for an interference from the Fe  $K_\beta$ .

**Results:** Figure 1a shows the Ni traverse of the right half of an M-shaped profile. The region between  $7\text{-}10\mu$  is clearly dominated by high-Ni metal, presumably because of the presence of tetrataenite. The highest Ni point indicates nearly pure tetrataenite (i.e., 50 wt.% Ni).

Figure 1b shows the profile for Co across the same traverse. Unlike Ni, which strongly partitions into kamacite, the Co “W-shaped” profile is smooth and less pronounced in the tetrataenite region than Ni, indicating either: (i) little affinity for tetrataenite over taenite, (ii) a faster diffusivity than Ni, or (iii) both.

Figure 1c shows the profile for Ge across the same traverse. Unlike the analyses of [4], we do not see an exact 1:1 correspondence between the shapes of the Ge and Ni profiles. This is presumably due to the higher special resolution of our analyses.

Two features in Fig. 1c are of interest:

(i) The Ge content of the kamacite and the distant taenite are in approximate agreement with an experimental  $^{68}\text{Ge}D_{\text{kam/tae}}$  of 1.1 [5] and Table 1. Therefore, through most of the kamacite growth, the kamacite and taenite appear to have communicated. However, also during this time, Ge has been transported to the tetrataenite region. So while sluggish Ni is piling up at the kamacite-taenite interface, mobile Ge is communicating  $10$ 's and even  $100$ 's of microns away [4]. Germanium is not being excluded from kamacite — it is *partitioning* into Ni-rich metal.

(ii) As noted above, the maximum Ge concentration in Fig. 1c does not exactly correspond to the maximum Ni concentration. We interpret this to mean that, towards the end of kamacite growth, Ge transport to the tetrataenite region was sluggish at the  $5\text{-}10\mu$  scale. From this we also infer that the diffusivity of Ge

was greater than that of Co, which was greater than that of Ni. The higher diffusivity ( $\mathcal{D}$ ) of Ge is consistent with experiments [8], but these same experiments indicate that diffusivities of Co and Ni should be very similar. We infer from this discrepancy between experiments and our analyses of Butler that low-temperature phase changes may be important for the interpretation of cooling rates.

Our new results are mainly consistent with previous traverse analyses of Ni, Co, and Ge in iron meteorites by [4,6]. The spatial resolution of our traverse is comparable to that of [6], who analyzed by nanoSIMS.

**Discussion: Cooling rates.** All of these observations appear to indicate that Ni diffusion becomes sluggish at higher temperatures than Ge. Our inference is that this sluggish behavior of Ni is due to a phase change that begins with the appearance of the  $\gamma_2$  FeNi phase at  $\sim 450^\circ\text{C}$  and conceivably continues as the ordered tetraetaenite phase forms at  $\sim 320^\circ\text{C}$  [3].

That said, given existing diffusivity data, we have doubts that even Ge was significantly mobile when tetraetaenite began to form. If the high-temperature ( $1350\text{-}1000^\circ\text{C}$ )  $^{\text{Ge}}\mathcal{D}$  of [7,8], which agree well, can be extrapolated to  $300^\circ\text{C}$ , then the diffusive scale length for Ge should be  $\sim 0.4\mu$  in 2 m.y., much too short for the equilibration distances of  $\sim 100\mu$  that appear to be observed in the Butler iron [4]. A more reasonable temperature for Ge mobility is  $\sim 500^\circ\text{C}$  where the regressed  $^{\text{Ge}}\mathcal{D}$  values predict a diffusive scale length of

$\sim 300\mu$  in 2 m.y. If so, our observations would then imply that the temperature at which Ni mobility effectively ceased would be  $\sim 500^\circ\text{C}$ . We have used 2 m.y. as a standard equilibration time in our calculations, but changing this to 10 m.y. will only change the equilibration distance by a factor of two.

**Natural and Experimental Partitioning.** Table 1 compares apparent partition coefficients from our Butler data with D's from [5,9]. Germanium and Co are the only elements where the observed and experimental kamacite/taenite D's agree closely. Our interpretation is that Ge and Co are elements whose  $\mathcal{D}$  are sufficiently large that kamacite and taenite can equilibrate over distances of  $\geq 100\mu$ . If kamacite and taenite cannot communicate, they cannot equilibrate.

**References:** [1] Wood J.A. (1964) *Icarus* **3**, 429–459. [2] Goldstein J.I. and Ogilvie R.E. (1965) *Trans. Met. Soc.* **233**, 2083–2087. [3] Goldstein J.I. et al. (2014) *Geochim. Cosmochim. Acta* **140**, 297–320. [4] Goldstein J.I. (1967) *J. Geophys. Res.* **18**, 4689–4696. [5] Janney P.E. and Jones J.H. (1990) *Lunar Planet. Sci. XXI*, 563–564. [6] Wasson J.T. and Hoppe P. (2012) *Geochim. Cosmochim. Acta* **84**, 508–524. [7] Narayan C. and Goldstein J. I. (1981) *Met. Trans.* **12A**, 1883–1890. [8] Righter K. et al. (2005) *Geochim. Cosmochim. Acta* **69**, 3145–3158. [9] Corrigan C.M. et al. (2009) *Geochim. Cosmochim. Acta* **73**, 2674–2691.

Table 1  
Apparent (Butler) and Experimental Partition Coefficients (D)

	D(tetra/kam)	D(tetra/tae)	D(kam/tae)	D(kam/tae) <sub>exp</sub>
Ni	10	2.8	0.28	$\sim 0.4^*$ , $0.83^{**}$
Co	0.18	$\sim 1?$	0.85	$0.98^{**}$
Ge	3.4	3.7	1.1	$1.2^*$ , $0.9^{**}$
Ga	$\sim 10$	$\sim 5$	$\sim 0.5$	$0.92^{**}$
Cu	$\sim 1.6$	$\sim 2$	$\sim 1.3$	$0.86^{**}$

\*[5]; \*\*[9]

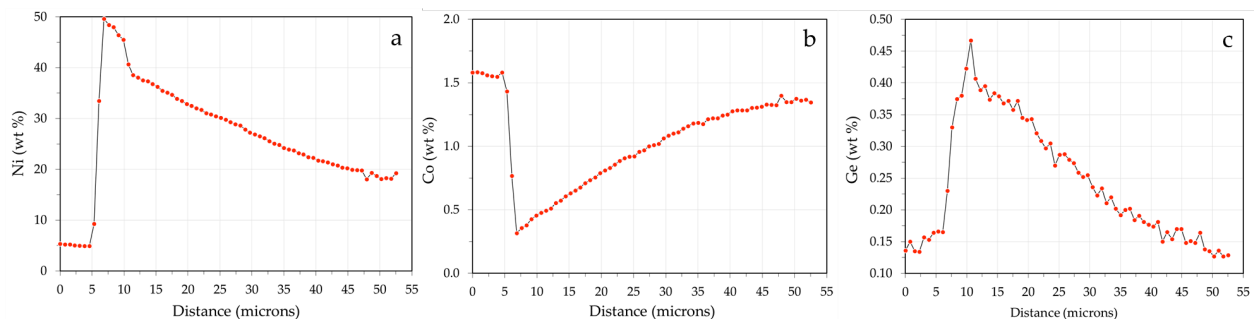


Figure 1. Compositional profiles across Kamacite-Taenite pair in Butler ungrouped iron.